Effect of particle size on the mechanism controlling n-hexane sorption in glassy polystyrene microspheres

D. J. Enscore, H. B. Hopfenberg and V. T. Stannett
Department of Chemical Engineering, North Carolina State University, Raleigh, North Carolina, 27607, USA
(Received 12 December 1976; revised 11 March 1977)

The effect of particle size on the rate-determining transport mechanism controlling n-hexane sorption into polystyrene spheres was determined by monitoring the kinetics of n-hexane vapour absorption in two powder samples of distinctly different narrow particle size distributions. The microspheres differed in mean diameter by a factor of three hundred. In all cases, sorption in the smaller spheres was controlled principally by Fickian diffusion. In contrast, at temperatures and activities which result in relaxation-controlled (Case II) transport in films, the larger spheres (184 μm diameter) sorb by Case II kinetics. Under these identical boundary conditions, however, the small spheres (5340 Å diameter) absorbed n-hexane by Fickian kinetics. Presumably, there is insufficient time or space in the small spheres to develop the step concentration profiles associated with limiting Case II transport. A mathematical model describing Case II sorption in spheres cylinders, and slabs is developed. The kinetics describing absorption in the larger spheres are well described by this analysis. Desorption in all cases is adequately described by concentration-dependent diffusion. Repeated experiments confirmed, moreover, that at identical temperatures and penetrant vapour activities the apparent equilibrium concentration of n-hexane in the small spheres is significantly higher than the corresponding sorption equilibria in the large spheres. Although several possible explanations for this glassy-state anomaly are presented, the most satisfying explanation involves the development of a non-sorbing core in the large spheres consequent to the prior sorption in the surrounding shell. Desorption data are consistent with the notion of partial swelling of large spheres.

INTRODUCTION AND DEVELOPMENT OF DESCRIPTIVE MODEL

Transport mechanisms of organic penetrants in glassy polymers

Most published research up to 1950 describing the interaction with and transport of penetrants in organic polymers was concerned with diffusional transport in rubbery polymers. A rather consistent transport mechanism, involving solution of penetrant in the polymer followed by Fickian diffusion through the polymer, characterizes virtually all of these many rubbery polymer–penetrant systems[1]. Small deviations from this diffusion model are encountered for rubbery systems confounded by crystalline regions which are susceptible to reordering by an interacting or plasticizing vapour or liquid penetrant.

The transport of organic molecules in glassy polymers often does not fit the Fickian diffusion model. Fickian diffusion is often encountered in glassy polymers for sorption at low activities and for desorption[2]. Sorption data, not explainable by the Fickian model, are usually termed 'anomalous diffusion'.

Alfrey, Gurnee and Lloyd[3] have presented a second limiting case for sorption in polymers in which the rate of transport is entirely controlled by polymer relaxations. This transport mechanism is designated Case II in contrast to Fickian diffusion which is termed Case I. Case II transport is characterized by the following features:

(a) As the solvent penetrates into the polymer, a sharp advancing boundary separates the glassy inner core from the swollen shell.

(b) The boundary between the swollen gel and the glassy core advances toward the film mid-plane at a constant velocity.

(c) The initial weight gain of the polymer sample is directly proportional to time.

(d) The swollen gel behind the advancing front is at a uniform state of swelling.

The introduction of the Case II mechanism did not, however, explain all anomalous sorption effects. Alfrey, Gurnee and Lloyd[3] suggest that these more complicated effects may be caused by a superposition of the two limiting transport mechanisms. Hopfenberg and Frisch[4] give a qualitative description of the various types of transport behaviour occurring in a glassy polymer/organic penetrant system over a wide range of temperature and penetrant activity. They present a generalized plot of a temperature–activity plane showing the various transport mechanisms.

A recent paper by Vrentas, Jarzebski and Duda[5] attempts to quantify the results of Hopfenberg and Frisch regarding the various types of transport encountered in amorphous polymer–penetrant systems. Vrentas *et al.* define a dimensionless group termed the Deborah number for diffusion by analogy to the Deborah number for flow of viscoelastic fluids given by Astarita and Marrucci[6]. Like Hopfenberg and Frisch[4], Vrentas *et al.*[5] subtend regions of the temperature–activity plane by lines which separate the various regimes of sorption behaviour. The analysis of

Vrentas, Jarzebski and Duda[5] implies that for a polymer–penetrant pair, at certain temperatures and penetrant activities, the characteristic polymer dimension will influence the nature of the observed sorption behaviour.

Transport of organic penetrants in glassy polymeric microspheres

Fickian or Case I mathematics. The solution of Fick's law for several sets of boundary conditions for transport in a sphere is given by Crank[7]. For constant and fixed boundary conditions and a constant diffusion coefficient, the sorption and desorption kinetics in spheres are given by:

$$M_t/M_\infty = 1 - \frac{6}{\pi^2}\sum_{n=1}^{\infty}\frac{1}{n^2}\exp(-Dn^2\pi^2 t/a^2) \qquad (1)$$

where M_t is the weight of penetrant sorbed at time t, M is the equilibrium weight of penetrant, a is the sphere radius, and D is the concentration-independent diffusion coefficient. An approximate solution to Fick's law at $M_t/M_\infty = 0.5$ gives a simple and useful relationship for calculation of $D(\mathrm{cm}^2/\mathrm{sec})$. Specifically:

$$D = \frac{0.00766\, d^2}{t_{1/2}} \qquad (2)$$

where $t_{1/2}$ is the diffusional half-time (sec), and d is the sphere diameter (cm). In this manner, a value for the diffusion coefficient can be obtained from the time required for one-half of the sorption to occur. It is possible to measure diffusion characterized by extremely low diffusion coefficients because of the small characteristic dimension obtainable in the spherical geometry.

Mathematical model describing Case II transport in spheres. Conversely, for penetration from high activity vapour or for liquid penetration of the sphere, absorption may be controlled by limiting Case II transport. The analysis presented here provides a useful model for describing limiting Case II transport in spheres and, in turn, permits calculation of an appropriate relaxation constant from observed integral sorption kinetics.

Consider the cross-section of the sphere undergoing Case II penetration. In the region $R \leqslant r \leqslant a$, where R is the radial position of the advancing sorption front and a is the sphere radius, there is a uniform concentration of penetrant equal to the equilibrium penetrant concentration, C_0. In the region $0 \leqslant r \leqslant R$, there is essentially no penetrant. There is, therefore, a discontinuity in concentration at the position $r = R$, corresponding to the position at which the rate-determining relaxations, controlling the overall kinetics, occur.

If k_0 is defined as the Case II relaxation constant (mg/cm^{2}min) and is assumed to be *constant* then the kinetic expression describing absorption into $N(a)$ uniform spheres of radius a is given by:

$$dM_t/dt = N(a)k_0 4\pi R^2 \qquad (3)$$

The amount of penetrant M_t absorbed in an array of uniform spheres in time t will be:

$$M_t = \frac{4\pi}{3}C_0 N(a)(a^3 - R^3) \qquad (4)$$

Since the rate-determining absorption step occurs at the position R, and the relaxations occur at an ever decreasing radius corresponding to an ever decreasing area, a continuously decreasing absorption rate dM_t/dt results from a kinetic process which is, in fact, zero-order in planar film geometries.

If one substitutes the mass balance, equation (4), into the kinetic expression, equation (3), one develops equation (5) consequent to the outlined algebraic simplifications:

$$\frac{d[4\pi C_0 N(a)(a^3 - R^3)]}{dt} = 3k_0 N(a)4\pi R^2 \qquad (5)$$

Cancelling yields

$$\frac{d(a^3 - R^3)}{dt} = 3\frac{k_0}{C_0}R^2$$

Differentiation and simplification provide:

$$dR/dt = (-k_0/C_0) \qquad (6)$$

Equation (6) justifies the intuitive notion that the relaxation front, positioned by the coordinate value R, moves toward the sphere centre with a velocity equal to the Case II relaxation constant, k_0, divided by the equilibrium penetrant concentration, C_0.

The algebraic relationship for R as a function of time is, therefore, given by:

$$R = a - (k_0/C_0)t \qquad (7)$$

and is defined only for $0 \leqslant t \leqslant (C_0/k_0)a$.

Substituting equation (7) into equation (4) yields:

$$M_t = \frac{4\pi C_0 N(a)}{3}\left[a^3 - (a - \frac{k_0}{C_0}t)^3\right] \qquad (8)$$

and since

$$M_\infty = (4/3)\pi C_0 N(a)a^3 \qquad (9)$$

M_t/M_∞ reduces to:

$$M_t/M_\infty = 1 - (1 - k_0 t/C_0 a)^3 \qquad (10)$$

An expression for the half-time for Case II absorption results from substitution of 0.5 for the ratio M_t/M_∞ in equation (10) and solving for $t_{1/2}$ in terms of a, k_0, and C_0. The resulting expression is:

$$t_{1/2} = 0.2063\, a\, C_0/k_0 \text{ or } 0.10315\, d\, C_0/k_0 \qquad (11)$$

where $d = 2a$ is the sphere diameter.

This model can be generalized by performing similar algebraic steps on alternate geometries of interest:

$$1 - M_t/M_\infty = \left(1 - \frac{k_0 t}{C_0 a}\right)^N \qquad (12)$$

where a is the sample radius for cylindrical and spherical samples and the film half-thickness for planar samples. The exponent N is determined by sample geometry and has

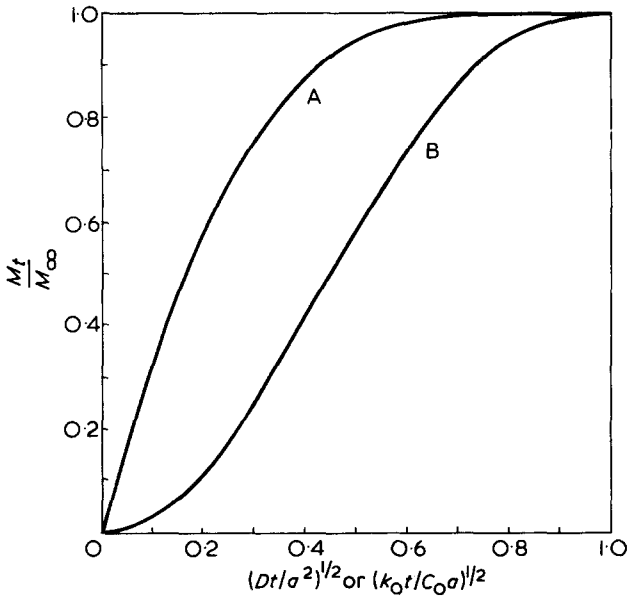

Figure 1 Generalized plots of dimensionless mass *versus* the square root of dimensionless time for: A, limiting Fickian (Case I); B, relaxation-controlled (Case II) penetration of a sphere

values of 1 for films, 2 for cylinders, and 3 for spheres.

Although the experimental results reported here will deal exclusively with spherical polymer particles, Case II behaviour has been observed in fibres and films. The data reported in the literature for fibres, however, have not in general been recognized explicitly as limiting Case II transport. For example, Watt's[8] data describing water transport in keratin fibres appear to be well described[9] by equation (12). However, the complex morphology and strong hydrogen bonding present in keratin fibres make a simplistic interpretation suspect.

Experimental distinction between Case I and Case II transport. The ideal calculated Fickian and Case II sorption curves describing fractional amount sorbed as a function of the square root of time are shown in *Figure 1* according to equations (1) and (12) respectively. The abscissa is presented as the square root of a dimensionless time for Case I diffusion, Dt/a^2, and k_0t/C_0a for Case II relaxation. The shape of the curves is generally the same for both cases; a monotonic decrease in sorption rate from time zero to equilibrium is predicted. An explicit separation of limiting transport mechanisms is readily apparent, since the Fickian diffusion curve still exhibits a monotonic inflection-free approach to equilibrium while the Case II curve is clearly sigmoidal. Plotting sorption data as a function of the square root of time, therefore, provides valuable information for inferring the controlling transport mechanism.

The diameter dependence of the sorption half-time provides an additional method for distinguishing between Case I and Case II sorption kinetics in spheres. The half-time for Fickian diffusion is proportional to the square of the sphere diameter (see equation 2) while the half-time for Case II transport (see equation 12) is proportional to the sphere diameter. If well characterized samples of polymeric spheres of varying diameter are available, the diameter dependence of the sorption half-time will provide distinction between the limiting rate-controlling mechanisms.

These limiting transport mechanisms do not explain all transport data. Alfrey, Gurnee and Lloyd[3] suggest that transport behaviour not explainable in terms of these two mechanisms may be due to a relaxation process occurring concurrently with a diffusional process. Berens[10] has reported sorption data for vinyl chloride monomer in poly(vinyl chloride) microspheres which, although essentially Fickian, are confounded by a slow approach to a final equilibrium. Berens and Hopfenberg[11] have proposed a model for this behaviour which combines Fickian diffusion and a first-order relaxation process. The sorption equation for this model is:

$$1 - M_t/M_\infty = \phi_F\left[\frac{6}{\pi^2}\sum_{n=1}^{\infty}\frac{1}{n^2}\exp(-4\pi^2 n^2 Dt/d^2)\right] + \phi_R\exp(-kt) \quad (13)$$

where D is the diffusion coefficient for the Fickian portion of the transport, k is the first-order relaxation constant, and ϕ_F and ϕ_R are the fractions of sorption contributed by Fickian diffusion and the relaxation respectively. If the diffusion kinetics are rapid relative to the relaxation kinetics, each of these constants can be determined empirically from the sorption data. On a semi-log plot of $(1 - M_t/M_\infty)$ *versus* linear time the long time slope would be $-k$ and the zero-time intercept of the long-time line is ϕ_R. The diffusion coefficient is calculated from the half-time associated with the purely Fickian contribution to the total sorption. Specifically, the half-time for diffusion is taken to be the time associated with an amount sorbed, $M_t = 0.5\ \phi_F\ M_\infty$ where $\phi_F = 1 - \phi_R$.

The microsphere geometry is ideally suited to the study of this type of transport. If the diffusion is much more rapid than the relaxation, it should be possible to observe a diffusional equilibration, followed by the long-term relaxation. This behaviour has been observed for the sorption of acetone and methanol in cellulose acetate films by Bagley and Long[12]. They were able to observe this behaviour in films because the diffusion coefficients for their system were four to five orders of magnitude higher than those for the VCM/PVC and n-hexane/polystyrene systems.

EXPERIMENTAL

Materials

Polystyrene microsphere samples. Microspheres of polystyrene in two diameter ranges were kindly prepared and characterized by the B. F. Goodrich Company Research and Development Center, Brecksville, Ohio. Four samples with diameters in the submicron range were prepared by emulsion polymerization. Four samples of polystyrene sphere, with diameters in the range 100–400 μm, were prepared by suspension polymerization at 70°C using 0.1 % w/w benzoyl peroxide as the initiator and poly(vinyl alcohol) as the dispersing agent. A 0.534 μm diameter emulsion-polymerized sample and a 184 μm diameter suspension-polymerized sample were selected for use in this investigation.

Organic penetrant. Pure (99 mol %) normal hexane, used as the penetrant in the vapour sorption experiments, was supplied by the Phillips Petroleum Company, Special Products Division, Bartlesville, Oklahoma. The n-hexane was used without further purification.

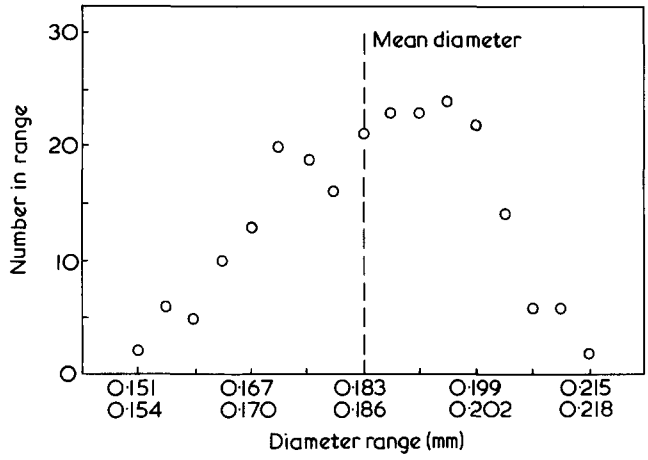

Figure 2 Particle size distribution for the large diameter polystyrene spheres

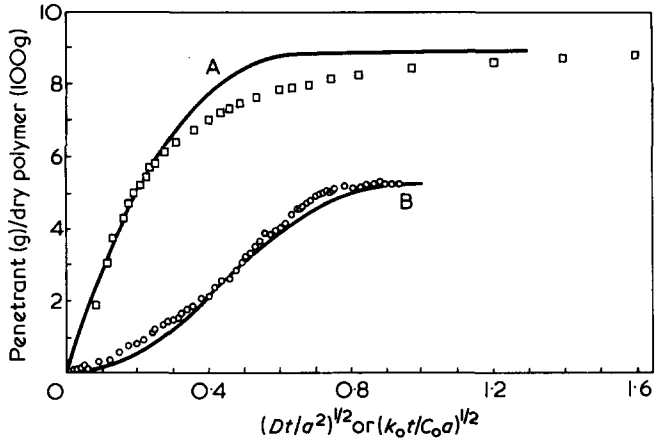

Figure 3 Comparison of theoretical curves and experimental data for n-hexane sorption into the large and small diameter polystyrene spheres at P/P_0 = 0.75 and 30°C. A, Fickian model, $D = 7.5 \times 10^{-14}$ (cm^2/sec); B, Case II model, $k_0 = 5.4 \times 10^{-6}$ (mg/cm^2 min). ○, d = 184 μm; □, d = 0.534 μm

Apparatus and procedure

Vapour sorption. These experiments were performed using a McBain spring balance system. The vapour sorption system was serviced by a high vacuum line for sample and penetrant degassing and desorption experiments. The temperature of the water jacketed sorption chamber was controlled to ±0.01°C by water circulated by a constant temperature bath. Helical quartz springs supplied by Worden Quartz Products Inc., Houston, Texas, were used to measure the amount of penetrant sorbed by the polystyrene samples. The springs extended linearly within 2% over the calibrated range and the sensitivity did not vary over the 10° to 50°C temperature range used in this investigation. The extension of the quartz spring was followed by an optical reader supplied by Misco Scientific, Berkeley, California. Desorption kinetics were routinely recorded after the n-hexane had sorbed to equilibrium. A more detailed discussion of the experimental procedure is given by Jacques and Hopfenberg[13,14].

Particle size distribution. The particle size distribution for the large spheres was determined by measuring the diameter of about 300 individual spheres optically using a Vickers microscope and a filar micrometer eyepiece. The particle size distribution for the large spheres is shown in *Figure 2*. The small spheres were characterized by the supplier using the Tyndall beam technique and electron microscopy.

RESULTS AND DISCUSSION

Sorption kinetics

A comparison of the experimentally determined kinetics of sorption is presented for the 184 μm diameter spheres and the 0.534 μm diameter spheres at an activity of 0.75 and a temperature of 30°C in *Figure 3*. The abscissa values were calculated by assuming a transport mechanism, based upon the form of the M_t *versus* $(t)^{1/2}$ data, and then calculating the appropriate kinetic constant, e.g. D (Case I) or k_0 (Case II) from the respective half-times. The curves presented in *Figure 3* were calculated using the respective mathematical model assuming Case II sorption for the large spheres and Fickian diffusion for the small spheres.

These experimental conditions, 30°C and P/P_0 = 0.75, are well within the range in which Jacques and Hopfenberg [13,14] observed Case II sorption of n-hexane in polystyrene films. The results presented here clearly indicate that Case II kinetics adequately describe the sorption of n-hexane into the large polystyrene spheres. Case II rate constants, k_0, calculated from all five large sphere sorption experiments are in excellent agreement with those reported for polystyrene films[14]. Specifically, the k_0 value calculated for the sorption kinetics at 45°C and a vapour activity of 0.75 in the large spheres is 4.53×10^{-5} mg/cm^2 min and the k_0 extrapolated from the data reported by Jacques and Hopfenberg[14] for sorption in films, under identical conditions, is 5.30×10^{-5} mg/cm^2 min.

In marked contrast, the Fickian diffusion model adequa-

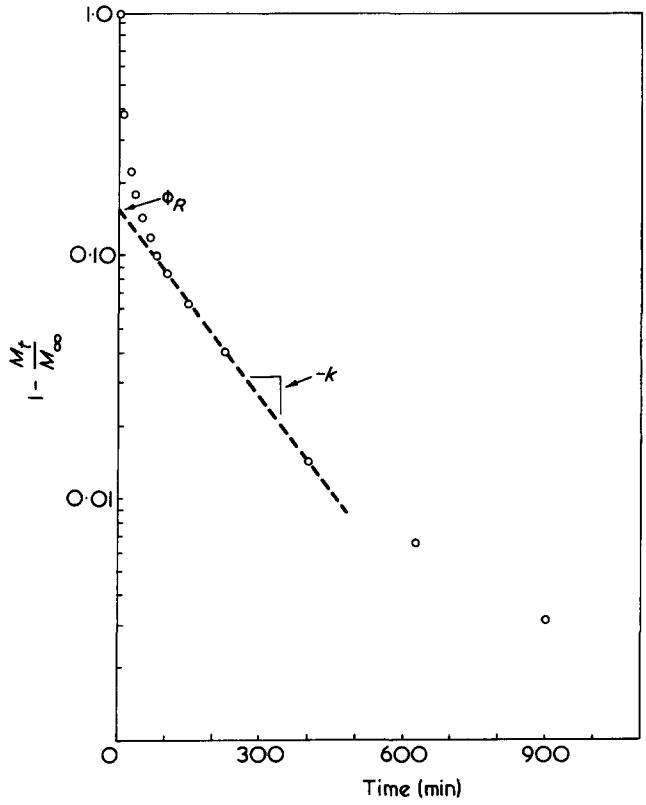

Figure 4 Plot of $1 - M_t/M_\infty$ *versus* linear time for n-hexane sorption into small diameter polystyrene spheres at P/P_0 = 0.75 and 30°C. D = 0.534 μm

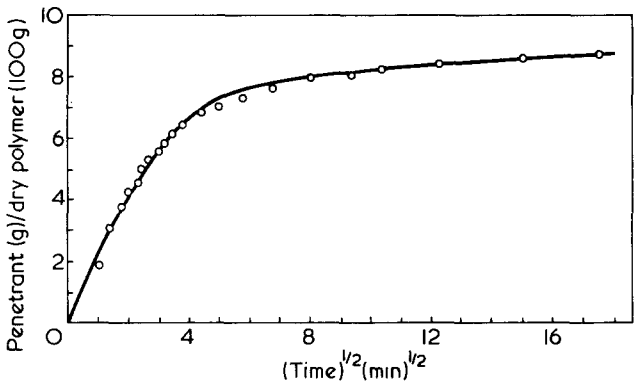

Figure 5 Comparison of Beren–Hopfenberg diffusion/relaxation model and experimental data for n-hexane sorption into the small polystyrene spheres at P/P_0 = 0.75 and 30°C. ○, Experimental data; ——, Berens–Hopfenberg model

tely describes sorption into the small spheres over approximately two-thirds of the total sorption. These data strongly suggest that diffusion into the small spheres is so rapid that there is insufficient time to generate a Case II concentration profile in these exceedingly small spheres. The extremely small diameter of the small spheres results in an experimentally determined half-time for sorption of only 4.8 min even though the corresponding diffusion coefficient is only 7.5 $\times 10^{-14}$ cm^2/sec. If the Case II mechanism were controlling, a half-time of 134 min for sorption into the small spheres would be predicted by equation (12) using values for relaxation constants, determined here for the large spheres and earlier by Jacques and Hopfenberg[14] for polystyrene films. Clearly the diffusional equilibration in the small spheres is essentially complete before the complex, step concentration profile associated with Case II sorption can be established.

Hopfenberg and Frisch[4] show that for a given polymer–penetrant system the rate-controlling transport mechanism is determined by the temperature and the penetrant activity. Vrentas, Jarzebski and Duda[5] suggest that for a given polymer–penetrant pair the characteristic size of a polymer sample may also be important in determining the controlling transport mechanism. The results of *Figure 3*, consistent with the earlier notions of Vrentas *et al.*[5], suggest that there is a critical sample diameter below which Case II transport does not apparently occur.

Although the early stages of sorption in the small spheres are diffusion-controlled the later stages of sorption are apparently controlled by a process that occurs over a much longer time interval. This two-stage sorption behaviour is quite similar to the observations of Berens[10] for the sorption of vinyl chloride monomer in poly(vinyl chloride) microspheres and, therefore, these sorption data were tested against the Berens–Hopfenberg diffusion/relaxation model[11]. The parameters for this model are conveniently calculated from the slope and intercept of the straight line portion of the $1 - M_t/M_\infty$ *versus* time plot presented in *Figure 6*. Data for sorption above $M_t/M_\infty = 0.99$ were not used because of the relative inaccuracy of the measurement of these small weight changes. The excellent fit of the experimental data to the Berens–Hopfenberg model is shown in *Figure 5*. It is not clear at present whether the relaxation process controlling later-stage sorption in the small spheres is related to that controlling Case II transport in the large spheres.

Equilibria

In addition to the marked difference in apparent kinetic mechanism controlling sorption, there is a significant difference in sorption equilibria between the large and small spheres. At an activity of 0.75 the small diameter spheres exhibit an equilibrium sorption of approximately 9 g of n-hexane per 100 g of dry polymer while the equilibrium concentration in the large diameter spheres is approximately 5 g/100 g. Jacques[13,14] reports an equilibrium concentration of 8.2 g/100 g for n-hexane sorption in polystyrene films at an activity of 0.75. The low equilibrium concentration was observed for all five sorption experiments on the 184 μm diameter spheres.

It is possible that subtle thermal and mechanical history effects could explain the difference in sorption equilibria between the large and small spheres. Berens[15,16] reports striking effects of sample history on sorption equilibria for the vinyl chloride/poly(vinyl chloride) system.

At a fixed vapour activity, the equilibrium concentration of n-hexane should vary with particle diameter owing to the effect of curvature on the hydrostatic pressure in the sphere[17]; however, this effect is small compared with the differences in equilibrium concentration observed here.

The small sphere equilibria agree with the sorption values observed in polystyrene films[13,14]. It is tempting to speculate that the large spheres did not reach equilibrium with the surrounding n-hexane vapour and that more swelling and vapour uptake would occur given sufficient time in contact with the penetrant. This long term sorption in the large spheres could, in fact, be extremely slow relative to the long term sorption in the small spheres, since each large sphere is seven orders of magnitude larger in volume than the 0.534 μm diameter spheres. The development of significant diffusional resistances in the rather thick outer shell of the large spheres could limit further sorption in the available experimental time.

However, the higher temperature sorption experiments were monitored for three days after the apparent equilibrium was reached and no further vapour uptake was observed. This experimental time corresponds to 1.4 (C_0a/k_0) or 40% longer than the equilibration time predicted by the Case II model. Typical results are presented for the large spheres sorbing at 45°C at an activity of 0.75 in *Figure 6*. The cor-

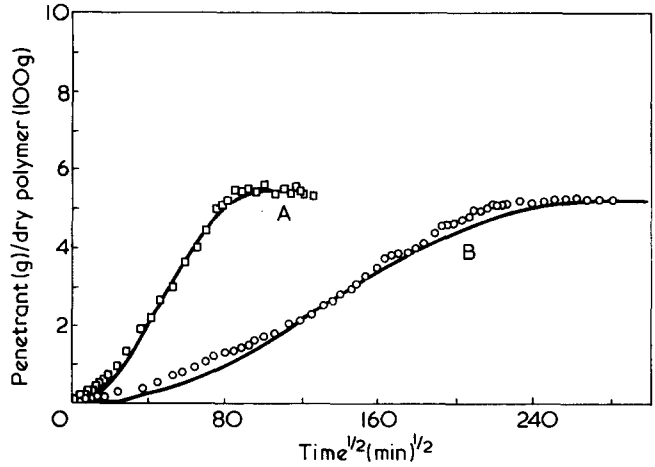

Figure 6 Comparison of theoretical curves and experimental data for n-hexane sorption into the large diameter polystyrene spheres at 30° and 45°C and P/P_0 = 0.75. A, 45°C; B, 30°C. ○, □, Experimental data; ——, Case II model. d = 184 μm

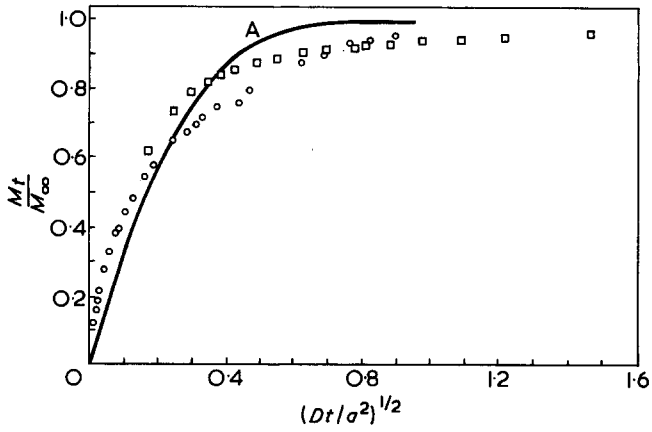

Figure 7 Comparison of theoretical curves and experimental data for n-hexane desorption from the large and small diameter polystyrene spheres at $P/P_0 = 0.75$ and 30°C. A, Fickian model. ○, d = 184 μm, $D = 4.5 \times 10^{-11}$ cm²/sec; □, d = 0.534 μm, $D = 1.4 \times 10^{-12}$ cm²/sec

responding sorption experiment at 30°C is also presented in *Figure 6.*

An hypothesis which explains the different sorption equilibria between the two sphere sizes is that sorption occurs only in the outer shell of the large spheres. This could be caused by either an inherent anisotropy in the large spheres or an anisotropy induced at some radial position by the prior swelling of the outer shell of the large spheres. This seems to be the most reasonable hypothesis and furthermore suggests a rather general effect which has not apparently been recognized previously. Clearly, if part of the large sphere is non-sorbing, a low apparent sorption equilibrium will be observed.

Even though a good fit with the experimental large sphere sorption data was obtained using the Case II model for a homogenous sphere, the spherical shell hypothesis is not ruled out. Since the Case II sorption front moves at a constant velocity in anisotropic or isotropic spheres, the Case II models do not *per se* discriminate effectively between limiting mechanisms for the two cases although the anisotropic model predicts a precipitous cessation of sorption. The deviations from the anisotropic sphere model (i.e. the rather gradual approach to a final equilibrium) observed at long times are consistent with realistic deviations from either original or swelling-imposed discontinuities at the final boundary between swollen and unswollen polymer.

Desorption kinetics

Microspheres previously equilibrated with n-hexane vapour at an activity of 0.75 and 30°C were subsequently exposed to a high vacuum at 30°C. A comparison of dimensionless fractional sorption, plotted against the square root of dimensionless time for diffusion, is presented for the large and small spheres in *Figure 7.* The diffusion coefficient values for desorption from the large and small spheres used in *Figure 7* are averages of diffusion of coefficients calculated using the half-time and long time methods. The dimensionless Fickian diffusion curve is also included in *Figure 7.* The Fickian diffusion model rather simplistically describes the desorption data since the Fickian model predicts a lower initial slope and a more rapid approach to the final equilibrium than the experimental data. This behaviour is, however, consistent with a strongly concentration-dependent diffusion coefficient[18].

At the same temperature, assuming uniformly swollen spheres, the diffusion coefficient calculated for desorption from the large spheres is two orders of magnitude higher than the diffusion coefficient characterizing desorption from the small spheres. This observation is entirely consistent with the hypothesis that sorption in the large spheres occurs only in the outer spherical shell. Specifically, if the same equilibrium concentration and inner core radius used to model Case II sorption into the spherical shell of the large spheres is used, desorption diffusion coefficients calculated from Crank's[7] solution to Fick's Law for hollow spheres correspond more closely to those describing desorption from the small spheres.

Data for n-hexane sorption and desorption in the small spheres at an activity of 0.018 and a temperature of 30°C are shown in *Figure 8.* Both the sorption and desorption kinetics appear to be Fickian, not confounded by long term relaxations. The slightly more rapid sorption is consistent with a concentration-dependent diffusion coefficient which varies monotonically with concentration. These results are gratifying since they confirm that the apparent long term drifts, observed at high penetrant activities, do in fact reflect relaxations rather than the effect of slowly sorbing large particles.

Calculated diffusion coefficients for sorption and desorption in the small spheres at a vapour activity of 0.75 over the temperature range used in this investigation are presented in *Figure 9.* At this activity, the diffusion coefficients for desorption from the small spheres are greater than the diffusion coefficients characterizing sorption into these same small spheres. The more rapid desorption is, quite possibly, a consequence of the prior swelling and distension of the microspheres which occurred during the long term relaxation of the polymer matrix. Bagley and Long[12] hypothesize that the long term sorption involves breaking of chain entanglements by osmotic pressure resulting in a more open polymer structure.

Activation energies

Sorption and desorption runs at, at least, three temperatures and a constant n-hexane activity of 0.75 were made for both sphere sizes. The activation energy for sorption into the large spheres was determined by calculating a Case II rate constant at each temperature. Assuming Arrhenius behaviour, for the Case II rate constants, the activation energy for Case II relaxation-controlled sorption into the large spheres was determined to be 25 kcal/g mol. The activation

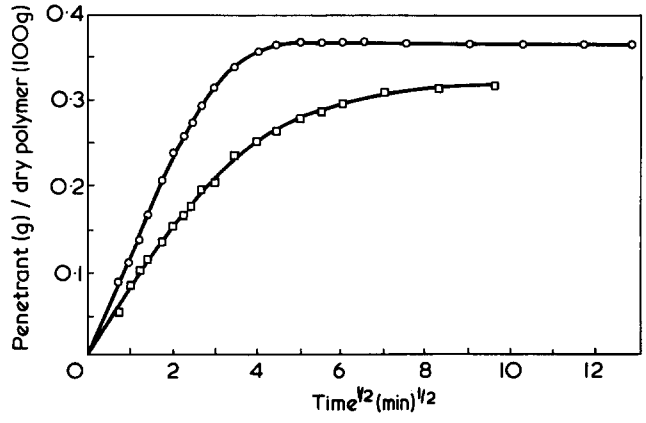

Figure 8 Data for n-hexane sorption in and desorption from the small polystyrene spheres at $P/P_0 = 0.018$ and 30°C. ○, Sorption; □, desorption. d = 0.534 μm

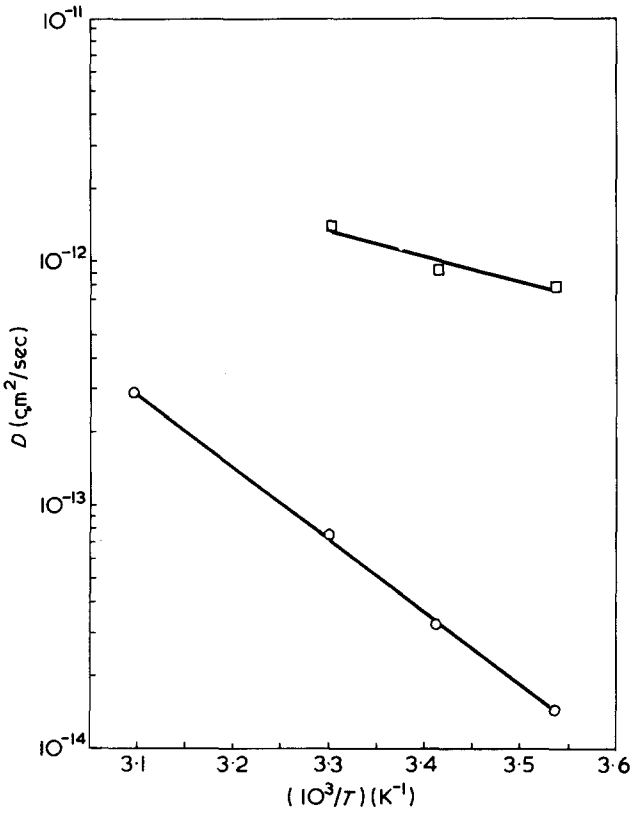

Figure 9 Arrhenius plots for n-hexane sorption in and desorption from the small diameter polystyrene spheres at $P/P_0 = 0.75$. □, Desorption; ○, sorption

energy for sorption into the small spheres and, similarly, for desorption from each sphere size was determined by calculating a diffusion coefficient at each temperature for each process. Assuming Arrhenius behaviour for the diffusion coefficients, the activation energy for diffusion in the small spheres was determined to be 13 kcal/g mol and the activation energies for diffusion during desorption from the large and small spheres were determined to be 10 and 5 kcal/g mol respectively. The Arrhenius plots of the respective kinetic constants are presented in *Figures 9* and *10*.

The activation energy for Case II transport, which is entirely relaxation-controlled, is higher than the activation energies for the Fickian transport processes. The higher activation energy for Case II transport is presumably related to the longer chain segments involved in relaxation of the polymer matrix compared with the segment lengths involved in penetrant diffusion in the polymer matrix. Interestingly, the activation energy of the sorption into the small spheres, which is controlled initially by diffusion and at long times by relaxation, lies between the activation energies for the two limiting processes.

CONCLUSIONS

Under conditions of temperature and penetrant activity where relaxation-controlled (Case II) transport is observed in films, the large diameter (184 μm) spheres also exhibit Case II transport. In marked contrast, sorption into the small diameter (0.534 μm) spheres, under identical boundary conditions, is largely controlled by Fickian diffusion for most of the sorption, followed by a smaller long term relaxation-controlled absorption. At much lower activities, purely Fickian sorption, uncomplicated by long-term relaxations, completely describes the observed transport kinetics in the small spheres.

A mathematical model describing Case II sorption in spheres, cylinders, and slabs is presented. The kinetics describing absorption in the larger spheres are well described by by this analysis. Similarly a mathematical model by Berens and Hopfenberg for diffusion coupled with relaxation in a sphere adequately describes the small sphere sorption data.

Repeated experiments confirmed, moreover, that, at identical temperatures and penetrant vapour activities, the apparent equilibrium concentration of n-hexane in the small spheres is significantly higher than the corresponding sorption equilibria in the large spheres. Although several possible explanations for this glassy-state anomaly are presented, the most satisfying explanation involves the development of a non-sorbing core in the large spheres consequent to the prior sorption in the surrounding shell.

Desorption data for both sphere sizes are described by Fickian diffusion with concentration-dependent diffusion coefficients. Additional support for the suggested controlling transport mechanisms is provided by the activation energies, which are 25 kcal/g mol for the relaxation-controlled sorption into the large spheres, 13 kcal/g mol for the partially relaxation-controlled sorption into the small spheres, and 10 and 5 kcal/g mol for diffusion-controlled desorption from the large and small spheres, respectively. For the small spheres the diffusion coefficient from highly swollen samples is larger for desorption than for sorption owing to the osmotic swelling of the polymer during the later stages of sorption. Diffusion coefficients calculated for the desorption kinetics from the large spheres are two orders of magnitude greater than the diffusion coefficients calculated for desorption from the small spheres. Presumably, this difference is a consequence of the incomplete penetration of the large spheres. If the diffusion coefficients characterizing desorption from the large spheres are calculated, assuming that the n-hexane sorbs in a shell surrounding an unpenetrated core, then the diffusion coefficients characterizing desorption in the large and small spheres are mutually consistent.

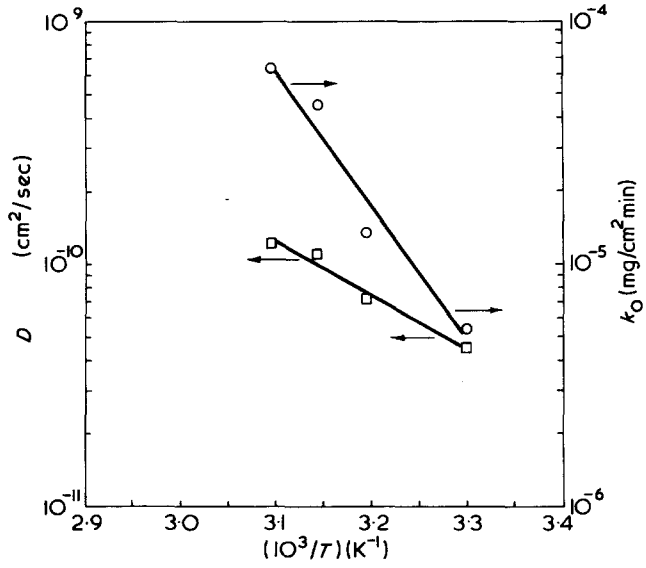

Figure 10 Arrhenius plots for n-hexane sorption in and desorption from the large diameter polystyrene spheres at $P/P_0 = 0.75$. □, Desorption; ○, sorption. $d = 184\mu m$

ACKNOWLEDGEMENTS

The authors wish to thank the Plastics Institute of America for the continued support provided to Mr David J. Enscore in the form of sequential Major Fellowship Awards. We are similarly grateful to Dr A. R. Berens and The B. F. Goodrich Company who provided us with the polymer microspheres and related characterizations. Moreover, Dr Berens significantly influenced our experimental and theoretical programme and stimulated our early interest in this problem. The support of the National Science Foundation through grant ENG75-22437 is gratefully acknowledged.

REFERENCES

1 Stannett, V. T. in 'Diffusion in Polymers', (Eds J. Crank and G. S. Park), Academic Press, London and New York, 1968, Ch 2
2 Hopfenberg, H. B. and Stannett, V. T. in 'The Physics of Glassy Polymers', (Ed. R. N. Haward), Wiley, New York, 1973, Ch 9
3 Alfrey, T. Jr, Gurnee, E. F. and Lloyd, W. G. *J. Polym. Sci. (C)* 1966, **12**, 249
4 Hopfenberg, H. B. and Frisch, H. L. *J. Polym. Sci. (B)* 1969, 7, 405
5 Vrentas, J. S., Jarzebski, C. M. and Duda, J. L. *AIChE J.* 1975, **21**, 894
6 Astarita, G. and Marrucci, G. 'Principles of Non-Newtonian Fluid Mechanics', McGraw-Hill, London, 1974
7 Crank, J. 'Mathematics of Diffusion', Oxford, London, 1956
8 Watt, I. C. *J. Appl. Polym. Sci.* 1964, **8**, 1737
9 Hopfenberg, H. B. and Enscore, D. J. unpublished results, 1976
10 Berens, A. R. *Polym. Prepr.* 1974, **15**, 203
11 Berens, A. R. and Hopfenberg, H. B. To be published
12 Bagley, E. and Long, F. A. *J. Am. Chem. Soc.* 1955, **77**, 2172
13 Jacques, C. H. M. and Hopfenberg, H. B. *Polym. Eng. Sci.* 1974, **14**, 441
14 Jacques, C. H. M. and Hopfenberg, H. B. *Polym. Eng. Sci.* 1974, **14**, 449
15 Berens, A. R. *2nd Int. Symp. PVC Lyons, France* July 1976
16 Berens, A. R. *Angew. Makromol. Chem.* 1975, **47**, 97
17 Vanzo, E., Marchessault, R. H. and Stannett, V. T. *J. Colloid Sci.* **20**, 62
18 Fujita, H. in 'Diffusion in Polymers, (Eds J. Crank and G. S. Park), Academic Press, London and New York, 1968, Ch 3